



Origin of the Hall-coefficient anisotropy in the Y–Al–Ni–Co periodic approximant to the decagonal phase

M. Komelj^a, J. Ivkov^b, A. Smontara^b, P. Gille^c, P. Jeglič^a, J. Dolinšek^{a,*}

^a J. Stefan Institute, University of Ljubljana, Jamova 39, SI-1000 Ljubljana, Slovenia

^b Institute of Physics, Laboratory for the Study of Transport Problems, Bijenička 46, POB 304, HR-10001 Zagreb, Croatia

^c Ludwig-Maximilians-Universität München, Department of Earth and Environmental Sciences, Crystallography Section, Theresienstrasse 41, D-80333 München, Germany

ARTICLE INFO

Article history:

Received 1 November 2008

Accepted 8 January 2009 by V. Pellegrini

Available online 16 January 2009

PACS:

61.44.Br

71.23.Ft

Keywords:

A. Complex intermetallics

A. Quasicrystalline approximants

D. Electronic transport

D. Hall effect

ABSTRACT

We present an experimental and theoretical study of the anisotropic Hall coefficient R_H of the Y–Al–Ni–Co periodic approximant to the decagonal phase with composition $\text{Al}_{76}\text{Co}_{22}\text{Ni}_2$. Performing *ab-initio* calculation of R_H for the original Y–Al–Ni–Co structural model [B. Zhang, V. Gramlich, W. Steurer, Z. Kristallogr. 210 (1995) 498] and its relaxed version, we reproduced the experimentally observed anisotropy for all combinations of crystalline directions of the electric current and magnetic field, where the relaxed model yielded better quantitative matching to the experiment. The origin of the anisotropic Hall coefficient is the anisotropic Fermi surface, the anisotropy of which originates from the specific stacked-layer structure of the Y–Al–Ni–Co compound and the chemical decoration of the lattice. Due to the structural similarity of Y–Al–Ni–Co to the *d*-Al–Ni–Co-type decagonal quasicrystals, the same physical picture explains the universal R_H anisotropy of this family of quasicrystals, where R_H changes sign along different crystalline directions.

© 2009 Elsevier Ltd. All rights reserved.

Decagonal quasicrystals (*d*-QCs) can be structurally viewed as a periodic stack of quasiperiodic atomic planes, so that *d*-QCs are two-dimensional quasicrystals, whereas they are periodic crystals in a direction perpendicular to the quasiperiodic planes. A consequence of the anisotropic structure are anisotropic electrical and thermal transport properties [1] (electrical resistivity, thermoelectric power, Hall coefficient, thermal conductivity), when measured along different crystalline directions. The anisotropy of the Hall coefficient R_H of *d*-QCs is especially intriguing, being positive hole-like ($R_H > 0$) for the magnetic field lying in the quasiperiodic plane, whereas it changes sign to negative ($R_H < 0$) for the field along the periodic direction, thus becoming electron-like. This R_H anisotropy was reported for the *d*-Al–Ni–Co, *d*-Al–Cu–Co and *d*-Al–Si–Cu–Co and is considered to be a universal feature of *d*-QCs [2, 3]. The lack of translational periodicity within the quasiperiodic layers prevents any quantitative theoretical analysis of this phenomenon. The problem can be overcome by considering periodic approximant phases to the *d*-QCs that are characterized by large unit cells, which periodically repeat in space, but the structure of the unit cell closely resembles *d*-QCs. Atomic layers are again stacked periodically and the periodicity lengths along the stacking direction are almost identical to those along the periodic direction of *d*-QCs. Approximant phases thus offer valid comparison to

the *d*-QCs with the advantage that theoretical calculations for the approximants—being periodic solids—are straightforward to perform. Recently, the anisotropic physical properties (magnetic susceptibility, electrical resistivity, thermoelectric power, Hall coefficient and thermal conductivity) of the $\text{Al}_{76}\text{Co}_{22}\text{Ni}_2$ monoclinic approximant to the *d*-Al–Ni–Co decagonal phase, known as the Y-phase of Al–Ni–Co (denoted as Y–Al–Ni–Co), were reported [4]. The Y–Al–Ni–Co phase [5] contains two atomic layers within one periodic unit along the stacking direction and its Hall coefficient R_H shows the same anisotropy as the *d*-Al–Ni–Co-type *d*-QCs. Searching for the microscopic origin of this anisotropy, we performed *ab-initio* calculation of the anisotropic Hall coefficient for the original Y–Al–Ni–Co structural model by Zhang et al. [5] and its relaxed version. While both models reproduce the R_H anisotropy at a qualitative level, the relaxed model gives better quantitative matching to the experimental data. Our *ab-initio* results show that the R_H anisotropy is a consequence of the specific shape of the anisotropic Fermi surface of the Y–Al–Ni–Co, which originates from the anisotropic stacked-layer atomic structure of this compound. An improved structural model of the Y–Al–Ni–Co, a relaxed version of the Zhang et al. model [5], is another achievement of this paper. It the calculations, a comparison between the original and the relaxed model was carried out systematically.

The temperature-dependent anisotropic Hall coefficient $R_H^{ilm} = E_l/j_i B_m$ (with *i*, *l*, *m* denoting crystalline directions of the current j_i , Hall electric field E_l and magnetic field B_m) of our investigated

* Corresponding author. Tel.: +386 1 4773 740; fax: +386 1 4263 269.
E-mail address: jani.dolinsek@ijs.si (J. Dolinšek).

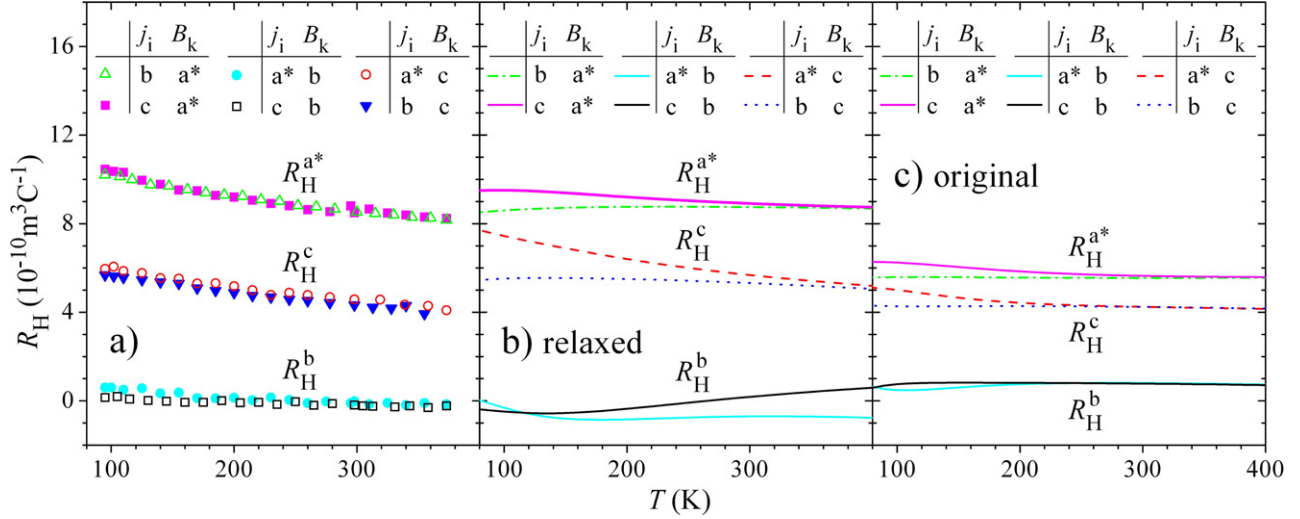


Fig. 1. (Color online) (a) Experimental anisotropic temperature-dependent Hall coefficient $R_H^{ilm} = E_l/j_i B_m$ of Y-Al-Ni-Co for different combinations of directions of the current j_i and magnetic field B_m (given in the legend). The superscript a^* , b or c on R_H denotes the direction of the magnetic field, whereas the indices i , l are omitted. (b) Theoretical anisotropic Hall coefficient for the same set of current and field directions as in (a). R_H was calculated *ab-initio* using the relaxed structural model of the Y-Al-Ni-Co phase of composition $\text{Al}_{75}\text{Co}_{25}$. (c) Theoretical anisotropic Hall coefficient calculated along the same lines as in (b), by using the original Zhang et al. [5] structural model of Y-Al-Ni-Co.

Y-Al-Ni-Co, reproduced from Ref. [4] (where the experimental details are also given), is displayed in Fig. 1a. Three sets of experiments were performed with the current and field along different combinations of the a^* , b and c orthogonal crystalline directions of the Y-Al-Ni-Co monoclinic unit cell (where the (a, c) monoclinic planes are stacked along the b direction that corresponds to the periodic direction in d -QCs, and a^* is perpendicular to b and c), making six experiments altogether. For all combinations of directions, the R_H^{ilm} values are typical metallic in the range $10^{-10} \text{ m}^3 \text{ C}^{-1}$, showing weak temperature dependence. The six R_H^{ilm} sets of data form three groups of two practically identical R_H^{ilm} curves, where the magnetic field in a given crystalline direction yields the same R_H^{ilm} for the current along the other two crystalline directions in the perpendicular plane (i.e., $R_H^{ilm} = R_H^{ilm}$). For that reason we drop the indices i , l in the following and retain just the index m of the magnetic field direction. Thus, identical Hall coefficients were obtained for combinations $E_b/j_c B_{a^*} = E_c/j_b B_{a^*} = R_H^{a^*}$ with $R_H^{a^*}(300 \text{ K}) = 8.5 \times 10^{-10} \text{ m}^3 \text{ C}^{-1}$, $E_{a^*}/j_c B_b = E_c/j_{a^*} B_b = R_H^b$ with $R_H^b(300 \text{ K}) \approx 0$ and $E_b/j_{a^*} B_c = E_{a^*}/j_b B_c = R_H^c$ with $R_H^c(300 \text{ K}) \approx 4.5 \times 10^{-10} \text{ m}^3 \text{ C}^{-1}$. The two rather high positive values $R_H^{a^*}$ and R_H^c for the field lying in the (a, c) atomic plane and the almost zero value of R_H^b for the field along the perpendicular b direction reflect strong anisotropy of the Fermi surface that consists mostly of hole-like parts, whereas electron-like and hole-like parts are of comparable importance for the field perpendicular to the (a, c) plane.

A quantitative theoretical analysis of the anisotropic Hall coefficient requires knowledge of the anisotropic electronic band structure. The *ab-initio* calculation of the band structure $\varepsilon_{\vec{k},n}$ (where n is the band index) was performed within the framework of the density functional theory by applying Wien97 code [6], which adopts the full-potential linearized-augmented-plane-wave (FLAPW) method [7]. Calculations were based on the Y-Al-Ni-Co structural model by Zhang et al. [5], where we have replaced Ni atoms by Co (thus considering the composition $\text{Al}_{75}\text{Co}_{25}$ instead of the “Zhang” composition $\text{Al}_{75}\text{Co}_{22}\text{Ni}_3$). The partially occupied sites Al(6) and Al(6') were taken with probabilities 1 and 0, respectively. The muffin-tin radii around the atoms were 1.16 Å that yielded the basis-set energy cutoff parameter 10 eV. The \vec{k} -space summation was performed in terms of the modified tetrahedron

method [8]. We used 180 \vec{k} -points for the self-consistent cycle and 4320 \vec{k} -points in the full Brillouin zone (BZ) for the additional iteration, which was performed in order to obtain a dense mesh of the energy eigenvalues $\varepsilon_{\vec{k},n}$ required for the calculation of the temperature-dependent transport coefficients. The criterion for the self-consistency was the difference in the total energy after the last two iterations, being less than 1×10^{-4} Ry. Calculating the electronic density of states (DOS) for the Zhang et al. [5] model, we found that the forces on some of the atoms were as large as 170 mRy/Å, so that the structure is obviously not in equilibrium. To bring the atoms to their equilibrium positions, we performed structural relaxation as implemented in the ABINIT code [9], which was stopped after the forces on all atoms were less than 0.02 mRy/Å in the relaxed structure. The final atomic coordinates before and after the structural relaxation are given in Table 1. The DOS of the original and the relaxed model are presented in Fig. 2. The DOS is strongly dominated by the transition-metal 3d states and exhibits a modest pseudogap close to the Fermi level ε_F without any spikes. The calculated Fermi surface in the first BZ of the original and the relaxed model is displayed in Fig. 3, using the drawing program *xcrysden* [10]. The Fermi surface is contributed by eleven bands that cross ε_F , resulting in a significant complexity and highly anisotropic structure. The DOS and the Fermi surface of the relaxed model show modest, but significant difference to the corresponding quantities of the original model (reproduced here from Ref. [4]).

The theoretical Hall coefficient R_H^{ilm} was calculated by means of the Boltzmann semiclassical theory as implemented in the BoltzTraP code [11]

$$R_H^{ilm}(T, \mu) = \frac{E_l}{j_i B_m} = (\sigma)_{\alpha l}^{-1}(T, \mu) \sigma_{\alpha \beta m}(T, \mu) (\sigma)_{i \beta}^{-1}(T, \mu). \quad (1)$$

R_H^{ilm} is a product of transport tensors as functions of the temperature T and the chemical potential μ

$$\sigma_{\alpha \beta}(T, \mu) = \int \sigma_{\alpha \beta}(\varepsilon) \left(-\frac{\partial f_\mu(T, \varepsilon)}{\partial \varepsilon} \right) d\varepsilon, \quad (2)$$

and

$$\sigma_{\alpha \beta \gamma}(T, \mu) = \int \sigma_{\alpha \beta \gamma}(\varepsilon) \left(-\frac{\partial f_\mu(T, \varepsilon)}{\partial \varepsilon} \right) d\varepsilon, \quad (3)$$

Table 1

Fractional atomic coordinates (x, y, z) of the relaxed model of Y–Al–Ni–Co. The coordinates (x_Z, y_Z, z_Z) of the original model of Zhang et al. [5] are given for comparison. The labels of the atomic positions together with their Wyckoff positions and site symmetry follow the labeling of Ref. [5] and TM denotes transition metal.

Atom	Wyckoff position	Site symmetry	x	y	z	x_Z	y_Z	z_Z
TM(1)	4i	m	0.2895	0	0.2830	0.2840	0	0.2775
TM(2)	4i	m	0.9863	0	0.1573	0.9879	0	0.1792
Al(1)	2b	$2/m$	0	1/2	0	0	1/2	0
Al(2)	4i	m	0.5867	0	0.3762	0.5911	0	0.3976
Al(3)	4i	m	0.2619	0	0.6220	0.2485	0	0.6046
Al(4)	4i	m	0.1356	0	0.1952	0.1285	0	0.1617
Al(5)	4i	m	0.8097	0	0.1104	0.8001	0	0.1014
Al(6)	2c	$2/m$	0	0	1/2	0	0	1/2
Al(7)	4i	m	0.4201	0	0.2364	0.4138	0	0.2263

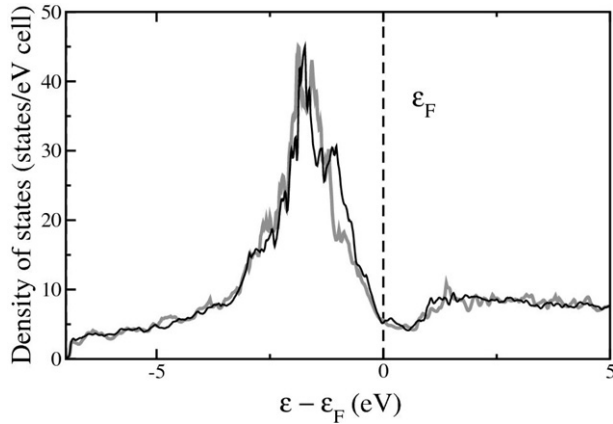


Fig. 2. Theoretical electronic DOS of the Y–Al–Ni–Co phase, calculated *ab-initio* for the original structural model of Zhang et al. [5] (thick grey curve) and the relaxed model (thin black curve), assuming composition $\text{Al}_{75}\text{Co}_{25}$. The DOS of the original model is reproduced from Ref. [4].

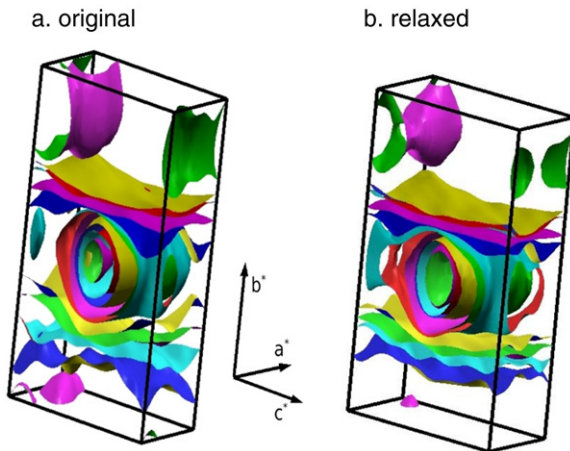


Fig. 3. (Color online) Fermi surface in the first Brillouin zone, calculated *ab-initio* for (a) the original Y–Al–Ni–Co model (Zhang et al. [5]) of composition $\text{Al}_{75}\text{Co}_{25}$ and (b) its relaxed version. Orientation of the reciprocal-space axes a^* , b^* and c^* is also shown. While a^* and c^* are perpendicular to b^* , the angle between a^* and c^* amounts 63.83° . The Fermi surface of the original model is reproduced from Ref. [4].

where $f_\mu(T, \varepsilon)$ is the Fermi–Dirac distribution. Since $-\partial f_\mu / \partial \varepsilon$ is a narrow bell-like function peaked at ε_F with the width of the order $k_B T$, this restricts the relevant energies entering Eqs. (2) and (3) to those in the close vicinity of the Fermi surface. The distributions $\sigma_{\alpha\beta}(\varepsilon)$ and $\sigma_{\alpha\beta\gamma}(\varepsilon)$ are the sums over the k points \vec{k} and bands n

$$\sigma_{\alpha\beta}(\varepsilon) = \frac{1}{\Omega} \sum_{\vec{k}, n} \sigma_{\alpha\beta}(\vec{k}, n) \delta(\varepsilon - \varepsilon_{\vec{k}, n}), \quad (4)$$

$$\sigma_{\alpha\beta\gamma}(\varepsilon) = \frac{1}{\Omega} \sum_{\vec{k}, n} \sigma_{\alpha\beta\gamma}(\vec{k}, n) \delta(\varepsilon - \varepsilon_{\vec{k}, n}), \quad (5)$$

where Ω is the unit-cell volume. The tensors

$$\sigma_{\alpha\beta}(\vec{k}, n) = \frac{\tau}{\hbar^2} \frac{\partial \varepsilon_{\vec{k}, n}}{\partial k_\alpha} \frac{\partial \varepsilon_{\vec{k}, n}}{\partial k_\beta}, \quad (6)$$

and

$$\sigma_{\alpha\beta\gamma}(\vec{k}, n) = \frac{e^3 \tau^2}{\hbar^4} \varepsilon_{\gamma\mu\nu} \frac{\partial \varepsilon_{\vec{k}, n}}{\partial k_\alpha} \frac{\partial \varepsilon_{\vec{k}, n}}{\partial k_\nu} \frac{\partial^2 \varepsilon_{\vec{k}, n}}{\partial k_\beta \partial k_\mu} \quad (7)$$

depend on the relaxation time τ , which drops out from the expression for the $R_H^{ilm}(T, \mu)$. Here $\varepsilon_{\gamma\mu\nu}$ denotes the Levi–Civita tensor [12,13]. The theoretical Hall coefficient calculated along the lines described above is a function of T and μ . In our calculation, the chemical potential μ equals the Fermi energy obtained from the *ab-initio* calculation.

The theoretical anisotropic Hall coefficient of the original and the relaxed Y–Al–Ni–Co structural model, calculated for the same set of combinations of the current and field directions as the experimental ones in Fig. 1a, is shown in Fig. 1b, c. For both models, the six theoretical R_H^{ilm} sets of data form three groups of two similar R_H^{ilm} curves, where the magnetic field in a given crystalline direction yields similar values of the coefficient for the current along the other two crystalline directions in the perpendicular plane. There exist some temperature-dependent differences within each group, where the temperature dependence originates from the Fermi–Dirac function. At a quantitative level, the relaxed model (Fig. 1b) gives better matching of the theoretical R_H^{ilm} values to the experimental ones. At 300 K, the relaxed model yields $R_H^{cba*} \approx R_H^{bca*} = R_H^{a*} \approx 8.8 \times 10^{-10} \text{ m}^3 \text{ C}^{-1}$, which compares well to the experimental value $R_H^{a*} = 8.5 \times 10^{-10} \text{ m}^3 \text{ C}^{-1}$. The figures for the other four combinations of the current and field directions are theoretical $R_H^{bba^*c} \approx R_H^{b^*bc} = R_H^c \approx 5.5 \times 10^{-10} \text{ m}^3 \text{ C}^{-1}$ versus the experimental $R_H^c = 4.5 \times 10^{-10} \text{ m}^3 \text{ C}^{-1}$ and (taking the average of $R_H^{ca^*b}$ and $R_H^{a^*cb}$) theoretical $R_H^{ca^*b} \approx R_H^{a^*cb} = R_H^b \approx -0.3 \times 10^{-10} \text{ m}^3 \text{ C}^{-1}$ versus the experimental $R_H^b \approx 0$. The relaxed model thus reproduces reasonably well the anisotropy of the Hall coefficient at a quantitative level. The small differences between the theoretical and the experimental values very likely originate from the fact that the experiment was performed on the sample of composition $\text{Al}_{76}\text{Co}_{22}\text{Ni}_2$, whereas the calculation was performed for the composition $\text{Al}_{75}\text{Co}_{25}$. Likewise, the fact that the two data sets within each of the three groups are experimentally practically indistinguishable (i.e., $R_H^{ilm} \approx R_H^{ilm}$), whereas theoretically some temperature-dependent differences exist, can be attributed to the inevitable residual structural inhomogeneity of the macroscopic samples, which tends to average out the differences within each group. Considering the theoretical R_H^{ilm} values of the original model (Fig. 1c), the agreement to the experiment is less satisfactory (the theoretical 300 K values $R_H^{a*} = 5.6 \times 10^{-10} \text{ m}^3 \text{ C}^{-1}$, $R_H^c = 4.1 \times 10^{-10} \text{ m}^3 \text{ C}^{-1}$ and $R_H^b = 0.8 \times 10^{-10} \text{ m}^3 \text{ C}^{-1}$ versus the

experimental $R_H^{a*} = 8.5 \times 10^{-10} \text{ m}^3 \text{ C}^{-1}$, $R_H^c = 4.5 \times 10^{-10} \text{ m}^3 \text{ C}^{-1}$ and $R_H^b \approx 0$). While the theoretical R_H^c and R_H^b values of the original model still match the experimental values well, this is not the case for the R_H^{a*} value, where the relaxed model gives much better matching to the experimental R_H^{a*} .

The theoretical Hall coefficient, calculated *ab-initio* for the $\text{Al}_{75}\text{Co}_{25}$ composition of the Y–Al–Ni–Co phase thus reproduces well the experimental features of the anisotropic Hall coefficient. The relaxed version of the Zhang et al. [5] model reproduces the anisotropic Hall coefficient at a quantitative level for all six investigated combinations of directions of the electric current and magnetic field, whereas the original model gives less satisfactory matching to the experiment, the discrepancy being mainly in the R_H^{a*} element. The origin of the anisotropic Hall coefficient is the anisotropic Fermi surface, the anisotropy of which in turn originates from the specific stacked-layer structure of the Y–Al–Ni–Co compound and the chemical decoration of the lattice. The Y–Al–Ni–Co periodic approximant is structurally closely related to the *d*-Al–Ni–Co type *d*-QCs [14], all showing the structure of two atomic layers stacked in one periodic unit of 0.4 nm. This structural similarity results in a similar anisotropy of the Fermi surface of all these compounds, resulting in a universal anisotropy of the Hall coefficient for this type of *d*-QCs [2,3]. It is also worth mentioning that the use of the relaxed model is very likely the reason for better matching of the theoretical anisotropic Hall coefficient to the experimental data, in comparison to the theoretical prediction for the anisotropy of the resistivity of Y–Al–Ni–Co reported in Ref. [4], where the original model yielded qualitative, but not quantitative matching to the experiment.

Acknowledgement

This work was done within the activities of the 6th Framework EU Network of Excellence “Complex Metallic Alloys” (Contract No. NMP3-CT-2005-500140).

References

- [1] J. Dolinšek, P. Jeglič, M. Komelj, S. Vrtnik, A. Smontara, I. Smiljanić, A. Bilušić, J. Ivkov, D. Stanić, E.S. Zijlstra, B. Bauer, P. Gille, Phys. Rev. B 76 (2007) 174207, and references therein.
- [2] Wang Yun-ping, Zhang Dian-lin, L.F. Chen, Phys. Rev. B 48 (1993) 10 542.
- [3] Zhang Dian-lin, Lu Li, Wang Xue-mei, Lin Shu-yuan, L.X. He, K.H. Kuo, Phys. Rev. B 41 (1990) 8557.
- [4] A. Smontara, I. Smiljanić, J. Ivkov, D. Stanić, O.S. Barišić, Z. Jagličić, P. Gille, M. Komelj, P. Jeglič, M. Bobnar, J. Dolinšek, Phys. Rev. B 78 (2008) 104204.
- [5] B. Zhang, V. Gramlich, W. Steurer, Kristallogr. 210 (1995) 498.
- [6] P. Blaha, K. Schwarz, P. Sorantin, S.B. Trickey, Comput. Phys. Commun. 59 (1990) 399.
- [7] E. Wimmer, H. Krakauer, M. Weinert, A.J. Freeman, Phys. Rev. B 24 (1981) 864.
- [8] P.E. Blöchl, O. Jepsen, O.K. Andersen, Phys. Rev. B 49 (1994) 16223.
- [9] X. Gonze, J.-M. Beuken, R. Caracas, F. Detraux, M. Fuchs, G.-M. Rignanese, L. Sindic, M. Verstraete, G. Zerah, F. Jollet, et al., Comput. Mater. Sci. 25 (2002) 478, the ABINIT computer program is a common project of the Université Catholique de Louvain, Corning Incorporated, and other contributors URL: <http://www.abinit.org>.
- [10] A. Kokalj, Comp. Mater. Sci. 28 (2003) 155. code available from <http://www.xcrysden.org>.
- [11] G.K.H. Madsen, J. Singh, Comput. Phys. Comm. 175 (2006) 67.
- [12] C.M. Hurd, The Hall Effect in Metals and Alloys, Plenum Press, New York, London, 1972.
- [13] H.J. Weber, Essential Mathematical Methods for Physicists, Elsevier Academic Press, San Diego, USA, 2004.
- [14] W. Steurer, T. Haibach, B. Zhang, S. Kek, R. Lück, Acta Crystallogr. B 49 (1993) 661.